RAD50 predicts the prognosis of hepatitis B virus-related hepatocellular carcinoma

Wangrui Liu
Youjiang Medical University for Nationalities
Wenhao Xu
Fudan University
Yuyan Chen
Affiliated Hospital of Nantong University
Xiaolei Sun
Nantong University
Liugen Gu
Nantong City No 1 People's Hospital and Second Affiliated Hospital of Nantong University
Yuanyuan Qu
Fudan University
Jingxin Zhang
Affiliated Hospital of Jiangsu University
Haineng Huang
Youjiang Medical University for Nationalities
Hailiang Zhang
Fudan University
Dingwei Ye
Fudan University
Xiaojuan Liu (lxj@ntu.edu.cn)
Nantong University https://orcid.org/0000-0001-7577-2943

Research article

Keywords: RAD50; hepatitis B virus; hepatocellular carcinoma

Posted Date: July 24th, 2019

DOI: https://doi.org/10.21203/rs.2.11886/v1

Abstract

RAD50, which is involved in the DNA double-strand break (DSB) repair process, is also involved in cancer outcomes. However, its role in hepatitis B virus (HBV)-associated hepatocellular carcinoma (HCC) remains unclear. RAD50 increased in HCC tissues compared to normal tissues and was correlated with OS in the TCGA cohort. The validation analysis indicated that increased RAD50 was expressed in HCC tissues in the two independent cohorts, 107 and 100 patients from the Affiliated Hospital of Youjiang Medical University of Nationalities (AHYMUN) and the Affiliated Hospital of Nantong University (AHNTU), respectively. In addition, HCC patients with elevated RAD50 expression showed poor OS and DFS in the AHYMUN cohort and decreased OS and DFS in the AHNTU cohort. Furthermore, four datasets obtained from the Oncomine database validated the analysis of the differential expression of RAD50 in HCC tumors and normal tissues. In conclusion, our study reveals that elevated RAD50 expression is correlated with cancer progression and poor survival in HBV-related HCC patients. These data suggest that RAD50 may act as an oncogene and may serve as a promising therapeutic target for HCC patients.

1. Introduction

In China, the incidence and mortality of primary hepatocellular carcinoma (HCC) is the second highest of all malignant cancers (1). In addition, in China, because the incidence of hepatitis B virus (HBV) infection is high, HBV accounts for at least 80% of HCC cases. In the Guangxi Zhuang Autonomous Region (2) and Qidong in Nantong Prefecture (3), HBV infection is very common, leading to a high incidence of HCC (4, 5). Although alpha-fetoprotein (AFP) and other markers have been widely used in clinical practice, the accuracy and sensitivity of diagnosis and targeted therapy need to be improved. Therefore, to reduce the cost of treatment for patients with HCC and to improve their quality of life, it is important to understand the underlying molecular mechanisms and apply them to the development of targeted treatments.

The DNA repair component protein Rad50 (RAD50) is a component of the MRN complex, which is a heterotrimer composed of RAD50, meiotic recombination 11 (MRE11), and Nijmegen fracture syndrome 1 (NBS1), that participates in the DNA damage response (DDR). Increased RAD50 expression is associated with multiple tumours, including breast cancer, ovarian cancer, lung cancer and rectal cancer (6-9). For example, RAD50 increases in colorectal cancer patients have been shown to be related to tumour development and prognosis (10). It is speculated that the high expression of RAD50 leads to cell instability, which increases the tendency toward DNA damage accumulation and malignant transformation. Following HBV infection, RAD50 expression in hepatocytes has been shown to be increased (11).

To investigate the expression and prognostic value of RAD50 in HCC, we recruited 207 HCC patients from two centres with confirmed pathological evidence of HCC. The prognostic role of RAD50 in HCC patients was validated and functionally annotated *in silico*. We speculate that RAD50 is associated with poor prognosis and may serve as a potential therapeutic target for HCC.

2. Materials And Methods

2.1. Patients and Variables

In this study, a total of 107 HCC patients were recruited from the Affiliated Hospital of Youjiang Medical University of Nationalities (AHYMUM) (Youjiang, China) between April 2008 and October 2018, and 100 HCC patients were also recruited from the Affiliated Hospital of Nantong University (AHNTU) (Nantong, China) for analyses between July 2013 and May 2017. The inclusion criteria consisted of the following: (1) HCC diagnosed by pathology (surgery or biopsy), typical dynamic imaging studies, and alpha fetoprotein serology according to the American Association for the Study of Liver Diseases (AASLD) guidelines [17]; (2) chronic viral hepatitis B infection [hepatitis B surface antigen (+)]; (3) no previous oncological treatment or liver resection; (4) no tumour invasion in the branches or trunk of the portal vein or hepatic veins according to MRI; (5) no other diffuse liver disease, including primary sclerosing cholangitis or primary biliary cirrhosis. The clinical and pathological parameters in the two cohorts, including age at surgery, gender, tumour size, AJCC stage, primary tumour lesion, the degree of pathological nuclear differential expression, Okuda score, albumin level, bilirubin level, presence of liver cirrhosis, and the degrees of microvascular invasion and capsular invasion are summarized in Table 1. Tissue samples, including HCC and adjacent normal tissues, were collected during surgery and were available from the AHYMUM and AHNTU tissue banks. All study designs and test procedures were performed in accordance with the Helsinki Declaration II. Ethical approval and consent to participate in the current study were obtained from the ethics committee.

2.2. Immunohistochemistry (IHC)

Immunostaining of RAD50 was performed using a mouse monoclonal anti-RAD50 antibody (1:1000, Ab89, Abcam, USA). Positive or negative staining of a specific protein on one FFPE slide was independently assessed by two experienced pathologists and determined according to the following description. The staining intensity level was graded from 0 to 3. Samples with no staining or weak, median or strong staining were graded at the level of 0, 1, 2 or 3, respectively. The staining extent ranged from 0 to 4 based on the percentage of coverage of the immunoreactive tumour cells (0%, 1-25%, 26-50%, 51-75%, or 76-100%, respectively). The overall IHC score, which was graded on a scale from 0 to 12, was generated by multiplying the staining intensity and extent scores. Negative staining was indicated by a grade from 0 to 3 and positive staining was indicated by a grade from 4 to 12 for each sample. All samples were classified into the tumour or normal group to confirm the differential expression of RAD50.

2.3. Statistical analysis

To determine the association of different RAD50 mRNA expression levels with clinicopathological characteristics, a $\chi 2$-test was performed to compare the distribution of the categorical data between groups. A scatter plot was utilized to represent the differential expression of RAD50 in normal and prostate cancer tissues. The primary end point was overall survival (OS) for patients who survived for a specific period of time, which was determined according to the length of time from the date of surgery to

the date of death or date of last follow-up. Disease-free survival (DFS), as the secondary end point, was defined as the length of time from the initiation of curative treatment when no disease could be detected until the date of progression, the initiation of second-line treatment or the date of death, whichever occurred first. The follow-up duration was estimated using the Kaplan-Meier method with a 95% CI and a log-rank test with separate curves. The hazard ratios were derived from Cox proportional hazard regression models based on a high-versus-low comparison to identify the independent predictors. Univariate and multivariate Cox regression models were independently analysed to evaluate the influence of the confounding covariates, including age at surgery, gender, tumour size, AJCC stage, primary tumour site, the degree of pathological nuclear differential expression, Okuda score, albumin level, bilirubin level, presence of liver cirrhosis, presence of microvascular invasion, presence of capsular invasion, and RAD50 expression, on survival. Statistical analyses were performed with SPSS software (version 23.0, SPSS Inc., Chicago, IL, USA). All hypothetical tests were two-sided, and P-values less than 0.05 were considered significant for all tests.

2.4. Determination of differential RAD50 expression based on Oncomine datasets

RAD50 expression profiles in hepatocellular tumour and normal tissue were analysed and displayed using the Oncomine online database (http://www.oncomine.com). A dataset including the known gene expression patterns in human HCC were included to validate the mRNA expression of RAD50 in the two groups. An unpaired t test was used to analyse the significant differences.

2.5. Data processing of Gene Set Enrichment Analysis (GSEA)

The Search Tool for the Retrieval of Interacting Genes (STRING; http://string-db.org) (version 10.0) online database was used to predict the PPI network for RAD50. Any interaction with a combined score >0.4 was considered statistically significant. The significant genes were included in functional and pathway enrichment analyses in a bubble chart using DAVID bioinformatics resources, which indicated the most significant signalling pathways according to GO and KEGG analysis. Datasets from the Cancer Genome Atlas (TCGA) database were analysed with the GSEA method using the category version 2.10.1 package in R. For each separate analysis, the Student's t-test statistical score was obtained for each of the consistent pathways, and the mean differential expression of each gene was calculated. A permutation test was performed 1000 times to identify the pathways with significant changes. The adjusted P values (adj. P), which were obtained by default using the Benjamini and Hochberg (BH) false discovery rate (FDR) method, were utilized to correct for the occurrence of false positive results. Significantly related genes were defined by an adj. P less than 0.01 and an FDR less than 0.25.

3. Results

In this study, the research was conducted in three steps. In the first step, the differential expression of RAD50 in normal and prostate tissues was analysed; in the second step, RAD50 expression in HCC patients was assessed as an indicator of progression and prognosis; in the third step, the differential

expression of RAD50 was validated in the Oncomine datasets, and GSEA was used to identify the relationships between significant genes and the involved signalling pathways.

3.1. Prognostic role of RAD50 in HCC based on TCGA

As shown in **Table 1**, in the AHYMUM cohort, increased RAD50 expression was significantly correlated with decreased age (p=0.021), advanced AJCC stage (p=0.001), the presence of multiple primary tumour lesions (p=0.001), the presence of microvascular invasion (p=0.028), the presence of capsular invasion (p=0.015), and increased Okuda score (p=0.009). In the AHNTU cohort, increased RAD50 expression was significantly associated with larger tumour size (p<0.001), advanced AJCC stage (p=0.003), the presence of multiple primary tumour lesions (p=0.010), the degree of pathological nuclear differential expression (p=0.005), the presence of microvascular invasion (p=0.001), the presence of capsular invasion (p=0.003), and higher Okuda score (p=0.008). A chi-square test showed that the baseline data were balanced in terms of the distribution of the categorical data, including gender, albumin level, bilirubin level and the presence of liver cirrhosis (p>0.05).

3.2. Expression of RAD50 in the AHYMUN and AHNTU cohorts

To analyse the RAD50 expression profile in HCC tissue, IHC was performed to reveal the staining distribution in tumour and normal tissues (**Fig. 2A**). The scatter plot of the IHC scores revealed that RAD50 expression was significantly elevated in HCC tissues in the AHYMUM (p<0.001) and AHNTU (p<0.001) cohorts (**Fig. 2B**).

3.3. Cox regression analyses

The univariate Cox regression analysis, as shown in the forest plots, revealed that age, gender, albumin level, bilirubin level and liver cirrhosis were not significantly associated with DFS in both AHYMUN (**Fig. 3A**) and AHNTU (**Fig. 3B**) patients. Meanwhile, tumour size was not a significant independent predictor of DFS in the AHYMUN cohort. In the multivariate models, the Okuda score (ref. I) was significantly associated with DFS in HCC patients, indicating the good representativeness of the population in the AHYMUN (HR: 1.914, p=0.045) and AHNTU (HR: 3.084, p=0.001) cohorts in the current study. More importantly, the subgroup analysis of RAD50 expression showed that RAD50 amplification was significantly correlated with DFS in the AHYMUN (HR: 4.612, p<0.001) and AHNTU (HR: 2.660, p=0.006) cohorts. Additionally, in the AHNTU cohort, a number of primary lesions was significantly correlated with poor DFS (HR: 2.563; p=0.007) according to the multivariate model used for the Cox regression analyses (**Table 2**).

In **Fig. 3C & D,** several parameters, including age, gender, albumin level, bilirubin level and the presence of liver cirrhosis, were not significantly associated with OS in the two cohorts. As shown in **Table 3**, the multivariate Cox analysis indicated that the Okuda score (ref. I) was significantly associated with OS in both the AHYMUN (HR: 2.329, p=0.031) and AHNTU (HR: 2.819, p=0.030) cohorts. RAD50 expression (ref. low) was significantly associated with OS in AHYMUM patients (HR: 6.807; p<0.001) but was not

markedly correlated with OS in HCC patients from the AHNTU (HR: 1.735; p=0.195) cohort. The other factors, including tumour size (ref.≤5 cm), the presence of multiple primary lesions (ref. single), the degree of pathological nuclear differential expression (ref. low), the presence of microvascular invasion (ref. absent) and the presence of capsular invasion (ref. absent), were not identified as prognostic indicators of OS in our study (p>0.05).

The survival curves suggested that HCC patients in the AHYMUN cohort with elevated RAD50 expression levels showed poor OS (p<0.001) and poor DFS (p<0.001) (**Fig. 4A & B**). In addition, in the AHNTU cohort, increased RAD50 expression was significantly associated with decreased OS (p=0.021) and DFS (p<0.001) (**Fig. 4C & D**).

3.4. Expression validation and GSEA

Four datasets (Rossler Liver 2 (12), Guichard Liver (13), Rossler Liver (12), and Chen Liver (14)) from the Oncomine database were analysed to validate the differential expression of RAD50 in HCC tumour and normal tissues (**Fig. 5**). A total of 11 significant genes, including *RAD51, ATM, XRCC6, RAD50, XRCC5, TERF2, ATR, MRE11A, BRAC1, NBN* and *TERF2IP*, were included in the molecular model shown in **Fig. 6A**. Functional and pathway enrichment analyses, including analyses of biological processes, cellular components, molecular functions and KEGG pathways, were performed using DAVID and are represented in the bubble chart in **Supplementary Fig. 1**. The significant and potentially related lncRNAs, targeted miRNAs and protein-protein interaction nodes are shown in **Fig. 6B**. Significant differences were found among the four validation datasets (p<0.05). A total of 100 significant genes were obtained from GSEA, and the genes with positive correlations were plotted. In addition, RAD50 was found to be involved in pathways from most functional annotation categories, including the nuclear body, ubiquitin ligase complex, G2M checkpoint and mitotic spindle signalling pathways. The details are shown in **Fig. 6**.

4. Discussion

In our study, we demonstrated that RAD50 was positively correlated with poor prognosis in HCC patients in the TCGA cohort. In the two validated cohorts, increased RAD50 expression was observed in cancer tissues compared to that in para-cancer tissues, which was shown be associated with decreased OS and DFS. Four validation cohorts from the Oncomine database also showed elevated RAD50 expression in HCC tissues compared with that in adjacent normal tissues. Additionally, the functional annotation bioinformatics analysis identified significant related hub genes and signalling pathways.

According to the IntAct molecular interaction database, human RAD50 potentially interacts with the transcription factor c-Jun/activator protein 1 (AP-1) (website: https://www.ebi.ac.uk/intact/interactors/id:Q92878*). C-Jun induces HBV-related liver tumourigenesis in mice via upregulating the transcription of its target gene osteopontin (OPN) (15). OPN is overexpressed in several human carcinomas and contributes to inflammation, tumour progression, and metastasis (16, 17). Therefore, we speculated that the interaction of RAD50 with c-Jun activated the transcription activity

of c-Jun, upregulated OPN expression, facilitated the development of HBV-related HCC, and contributed to poor prognosis.

Our study suggested that increased RAD50 expression in HBV-related HCC is a marker of poor prognosis. Aude Dupré and colleagues designed a chemical forward genetic screen to identify a small-molecule inhibitor of the MRN complex, named Z-5-(4-hydroxybenzylidene)-2-imino-1,3-thiazolidin-4-one (mirin) (18). In 2009, other researchers confirmed the structure of mirin (19). However, there have been no reports about the use of mirin in cellular, animal and clinical applications. We questioned whether mirin could be used in an HBV-related HCC animal model to determine the therapeutic effect of the inhibition of the MRN complex.

The predictive power of RAD50 may be as strong as that of the classical factors commonly used in clinical practice. Serum tumour markers are the most commonly used markers for the monitoring and early diagnosis of HBV-related HCC because they are non-invasive, objective, and reproducible. The most common serological test utilizes AFP. Disappointingly, in a retrospective case-control study, the sensitivity of AFP testing at the most effective cut-off value (10-20 ng/ml) in the diagnosis of HCC was approximately 60%, and its specificity was 80% (20, 21). These values are much lower than those required for the treatment and prediction of prognosis of HCC patients. However, RAD50 was shown to be a significant and independent biomarker (22). This means that it may be used to shed further light on the mechanisms underlying HCC progression, to facilitate the discovery of new therapies, and to open up new avenues for the personalized treatment of HCC patients.

In this study, the analysis of the data form the two cohorts supported our hypothesis and clearly demonstrated the high expression of RAD50 in tumour tissues from HCC patients, which results in increases in the HCC recurrence rate and poor overall survival. At the same time, GSEA indicated that RAD50 is involved in some of the most important pathways, including the mitotic spindle, UV response and transforming growth factor beta (TGF-β) signalling pathways, that are enriched in HCC specimens. In addition to participating in the DSB repair pathway, RAD50 also interacts with MMAP, which is expressed by the mitotic-specific MRN complex to maintain optimal genomic stability during mitosis (23).

The strength of our study is that we first attempted to study the role of RAD50 as a prognostic factor for HCC. The relationship between RAD50 and HCC has rarely been investigated (24). However, it is worth noting that RAD50 is a repair factor that has been identified in the DSB reaction and is highly expressed in many cancers. With this in mind, to further explain the role of RAD50 in the invasion and metastasis of HCC, we used GSEA to analyse data from public databases to identify important genes and pathways that may be involved in the relevance of RAD50 to the initiation of carcinogenesis.

The limitations of this study are as follows. First, the retrospective nature of the data set is obvious. Although data was obtained from two institutes at the Nantong University Affiliated Hospital and the Youjiang Nationalities Medical College Affiliated Hospital, the sample size is relatively small, and the patients in the two Chinese centres exhibit economic and geographical differences, which may lead differences in therapeutic strategies and overall prognoses. Second, while our research involved a

thorough functional annotation of RAD50 in HCC, we failed to confirm the underlying mechanisms. In the future, we will conduct multi-center research in Europe and the United States to further explore the role of RAD50 in the development and prognosis of HCC.

5. Conclusion

In conclusion, our study is the first to reveal that elevated RAD50 expression is significantly correlated with cancer progression and poor survival in HBV-related HCC patients. These data suggest that RAD50, which is a potential therapeutic target, may act as an oncoprotein and could serve as a promising prognostic marker in HCC patients. In this regard, randomized clinical trials and further investigation are required to identify the true value of RAD50 in terms of its clinical application in HCC patients.

List Of Abbreviations

HBV	hepatitis B virus
HCC	Hepatocellular carcinoma
DDR	DNA damage response
IHC	immunohistochemistry
AHYMUM	Affiliated Hospital of YouJiang Medical University for Nationalities
AHNTU	Affiliated Hospital of Nantong University
TCGA	the Cancer Genome Atlas
DFS	disease-free survival
OS	overall survival
HR	hazard ratio
CI	confidence interval

Declarations

Ethics approval and consent to participate: The ethics approval and consent to participate in the current study were obtained from the ethics committees of the AHYMUM and the AHNTU.

Consent for publication: Not applicable.

Availability of data and materials: The datasets and/or analysis results used during the current study are available from the corresponding author upon reasonable request.

Competing interests: The authors declare no competing interests.

Acknowledgments: This work is supported by grants from the National Natural Science Foundation of China (No. 81202004, 81802525, 81472377) and the Shanghai Natural Science Foundation of China (No. 16ZR1406400). This study was partly supported by the major project (No. MS22018009) and the general project (No. JC2018087) of Nantong city.

Authors' contributions: The work presented here was carried out with the collaboration of all authors. DW Ye and HL Zhang defined the research topic and discussed the analyses and their interpretation, and presentation. HN Huang and XJ Liu developed the algorithm, provided pathological samples, provided clinicopathological data and performed the statistical analysis. WH Xu, WR Liu and YY Chen drafted the manuscript, recorded the clinical data, analysed the IHC data and interpreted the results. LG Gu and LQ He collected clinical and pathological records and helped to analyse the IHC data. HK Wang and YY Qu participated in reviewing all clinical records and performed the associated data collection. All authors read and approved the final manuscript.

References

1. Chen JG, Zhang SW. Liver cancer epidemic in China: past, present and future. Seminars in cancer biology 2011; 21, 59-69. 2. Zheng D, Deng W, Huang T, Li X, Li Z. [Relationship between hepatitis B virus genotype, BCP/Pre-C region mutations and risk of hepatocellular carcinoma in Guangxi Zhuang Autonomous Region]. Zhonghua Liu Xing Bing Xue Za Zhi 2015; 36, 725-729. 3. Chen T, Qian G, Fan C, Sun Y, Wang J, Lu P, Xue X, Wu Y, Zhang Q, Jin Y, Wu Y, Gan Y, Lu J, Kensler TW, Groopman JD, Tu H. Qidong hepatitis B virus infection cohort: a 25-year prospective study in high risk area of primary liver cancer. Hepatoma Res 2018; 4. 4. Bei C, Tan C, Zhu X, Wang Z, Tan S. Association Between Polymorphisms in CMTM Family Genes and Hepatocellular Carcinoma in Guangxi of China. DNA Cell Biol 2018; 37, 691-696. 5. Fan C, Li M, Gan Y, Chen T, Sun Y, Lu J, Wang J, Jin Y, Lu J, Qian G, Gu J, Chen J, Tu H. A simple AGED score for risk classification of primary liver cancer: development and validation with long-term prospective HBsAg-positive cohorts in Qidong, China. Gut 2019; 68, 948-949. 6. Tommiska J, Seal S, Renwick A, Barfoot R, Baskcomb L, Jayatilake H, Bartkova J, Tallila J, Kaare M, Tamminen A, Heikkila P, Evans DG, Eccles D, Aittomaki K, Blomqvist C, Bartek J, Stratton MR, Nevanlinna H, Rahman N. Evaluation of RAD50 in familial breast cancer predisposition. Int J Cancer 2006; 118, 2911-2916. 7.

Zhang M, Liu G, Xue F, Edwards R, Sood AK, Zhang W, Yang D. Copy number deletion of RAD50 as predictive marker of BRCAness and PARP inhibitor response in BRCA wild type ovarian cancer. Gynecol Oncol 2016; 141, 57-64. 8. Adams DL, Adams DK, He J, Kalhor N, Zhang M, Xu T, Gao H, Reuben JM, Qiao Y, Komaki R, Liao Z, Edelman MJ, Tang CM, Lin SH. Sequential Tracking of PD-L1 Expression and RAD50 Induction in Circulating Tumor and Stromal Cells of Lung Cancer Patients Undergoing Radiotherapy. Clin Cancer Res 2017; 23, 5948-5958. 9. Ho V, Chung L, Singh A, Lea V, Abubakar A, Lim SH, Ng W, Lee M, de Souza P, Shin JS, Lee CS. Overexpression of the MRE11-RAD50-NBS1 (MRN) complex in rectal cancer correlates with poor response to neoadjuvant radiotherapy and prognosis. BMC Cancer 2018; 18, 869. 10. Gao J, Zhang H, Arbman G, Sun XF. RAD50/MRE11/NBS1 proteins in relation to tumour development and prognosis in patients with microsatellite stable colorectal cancer. Histol Histopathol 2008; 23, 1495-1502. 11. Ryu HM, Park SG, Yea SS, Jang WH, Yang YI, Jung G. Gene expression analysis of primary normal human hepatocytes infected with human hepatitis B virus. World J Gastroenterol 2006; 12, 4986-4995. 12. Roessler S, Jia HL, Budhu A, Forgues M, Ye QH, Lee JS, Thorgeirsson SS, Sun Z, Tang ZY, Qin LX, Wang XW. A unique metastasis gene signature enables prediction of tumor relapse in early-stage hepatocellular carcinoma patients. Cancer research 2010; 70, 10202-10212. 13. Guichard C, Amaddeo G, Imbeaud S, Ladeiro Y, Pelletier L, Maad IB, Calderaro J, Bioulac-Sage P, Letexier M, Degos F, Clement B, Balabaud C, Chevet E, Laurent A, Couchy G, Letouze E, Calvo F, Zucman-Rossi J. Integrated analysis of somatic mutations and focal copy-number changes identifies key genes and pathways in hepatocellular carcinoma. Nature genetics 2012; 44, 694-698. 14. Chen X, Cheung ST, So S, Fan ST, Barry C, Higgins J, Lai KM, Ji J, Dudoit S, Ng IO, Van De Rijn M, Botstein D, Brown PO. Gene expression patterns in human liver cancers. Molecular biology of the cell 2002; 13, 1929-1939. 15. Trierweiler C, Hockenjos B, Zatloukal K, Thimme R, Blum HE, Wagner EF, Hasselblatt P. The transcription factor c-JUN/AP-1 promotes HBV-related liver tumorigenesis in mice. Cell Death Differ 2016; 23, 576-582. 16. Weber CE, Kothari AN, Wai PY, Li NY, Driver J, Zapf MA, Franzen CA, Gupta GN, Osipo C, Zlobin A, Syn WK, Zhang J, Kuo PC, Mi Z. Osteopontin mediates an MZF1-TGF-beta1-dependent transformation of mesenchymal stem cells into cancer-associated fibroblasts in breast cancer. Oncogene 2015; 34, 4821-4833. 17. Qin X, Yan M, Wang X, Xu Q, Wang X, Zhu X, Shi J, Li Z, Zhang J, Chen W. Cancer-associated Fibroblast-derived IL-6 Promotes Head and Neck Cancer Progression via the Osteopontin-NF-kappa B Signaling Pathway. Theranostics 2018; 8, 921-940. 18. Dupre A, Boyer-Chatenet L, Sattler RM, Modi AP, Lee JH, Nicolette ML, Kopelovich L, Jasin M, Baer R, Paull TT, Gautier J. A forward chemical genetic screen reveals an inhibitor of the Mre11-Rad50-Nbs1 complex. Nat Chem Biol 2008; 4, 119-125. 19. Garner KM, Pletnev AA, Eastman A. Corrected structure of mirin, a small-molecule inhibitor of the Mre11-Rad50-Nbs1 complex. Nat Chem Biol 2009; 5, 129-130; author reply 130. 20. Marrero JA, Feng Z, Wang Y, Nguyen MH, Befeler AS, Roberts LR, Reddy KR, Harnois D, Llovet JM, Normolle D, Dalhgren J, Chia D, Lok AS, Wagner PD, Srivastava S, Schwartz M. Alpha-fetoprotein, des-gamma carboxyprothrombin, and lectin-bound alpha-fetoprotein in early hepatocellular carcinoma. Gastroenterology 2009; 137, 110-118. 21. Lok AS, Sterling RK, Everhart JE, Wright EC, Hoefs JC, Di Bisceglie AM, Morgan TR, Kim HY, Lee WM, Bonkovsky HL, Dienstag JL. Des-gamma-carboxy prothrombin and alpha-fetoprotein as biomarkers for the early detection of hepatocellular carcinoma. Gastroenterology 2010; 138, 493-502. 22. Chen C, Wang Y, Mei JF, Li SS, Xu HX, Xiong HP, Wang XH, He X. Targeting RAD50 increases sensitivity to radiotherapy in colorectal cancer cells.

Neoplasma 2018; 65, 75-80. 23. Xu R, Xu Y, Huo W, Lv Z, Yuan J, Ning S, Wang Q, Hou M, Gao G, Ji J, Chen J, Guo R, Xu D. Mitosis-specific MRN complex promotes a mitotic signaling cascade to regulate spindle dynamics and chromosome segregation. Proceedings of the National Academy of Sciences of the United States of America 2018; 115, E10079-e10088. 24. Jackson SP, Bartek J. The DNA-damage response in human biology and disease. Nature 2009; 461, 1071-1078.

Figure Legends

Fig.1. A: Kaplan-Meier survival analyses of different RAD50 expression groups based on OS in 423 patients with hepatocellular carcinoma from the TCGA database; B: Differential transcriptomic expression of RAD50 in tumour and normal tissues in the TCGA cohorts.

Fig.2. A: IHC staining of hepatocellular carcinoma and normal tissues from patients in the AHYMUN and AHNTU cohorts; B: Scatter plot showing the IHC scores derived from normal and tumour tissues ($p<0.001$) from different cohorts.

Fig.3. Forest plots were used to visualize the univariate Cox regression analysis of DFS and OS in the AHYMUM and AHNTU cohorts.

Fig.4. Kaplan-Meier survival analyses of different RAD50 expression groups based on OS and DFS in 107 patients with hepatocellular carcinoma from the AHYMUM cohort (A/B) and in 100 patients from the AHNTU cohort (C/D).

Fig.5. Analysis of expression in hepatocellular tumour vs. normal tissues based on data from the Oncomine database. (A) Roessler, et al., A unique metastasis gene signature enables prediction of tumor relapse in early-stage hepatocellular carcinoma patients, Cancer Res, 2010; (B) Guichard C, et al., Integrated analysis of somatic mutations and focal copy-number changes identifies key genes and pathways in hepatocellular carcinoma, Nature Genetics, 2012; (C) Roessler, et al., A unique metastasis gene signature enables prediction of tumor relapse in early-stage hepatocellular carcinoma patients, Cancer Res, 2010; (D) Chen X, et al., Gene expression patterns in human liver cancers, Mol Biol Cell, 2002.

Fig.6. Datasets from the TCGA database were analysed with the GSEA method. For each separate analysis, a Student's t-test was performed to obtained the statistical scores from the consistent pathways, and the means of the differential expression of genes were calculated. A permutation test was

performed 1000 times to identify the significantly changed pathways. The adjusted P values (adj. P) were generated using the Benjamini and Hochberg (BH) false discovery rate (FDR) method by default and were used to correct for the occurrence of false positive results. Significantly related genes were defined by an adj. P less than 0.01 and an FDR less than 0.25. The most significant highly involved pathways included the nuclear body, ubiquitin ligase complex, G2M checkpoint and mitotic spindle pathways.

Supplementary Fig.1. A total of 11 significant genes, including RAD51, ATM, XRCC6, RAD50, XRCC5, TERF2, ATR, MRE11A, BRAC1, NBN and TERF2IP, were identified in the molecular model shown in Fig. 5A. Functional and pathway enrichment analyses were performed using DAVID to obtain a bubble chart. The GO analysis of biological processes, cellular components, and molecular functions and the KEGG analysis of the DEGs indicated the most significant signalling pathways.

Figures

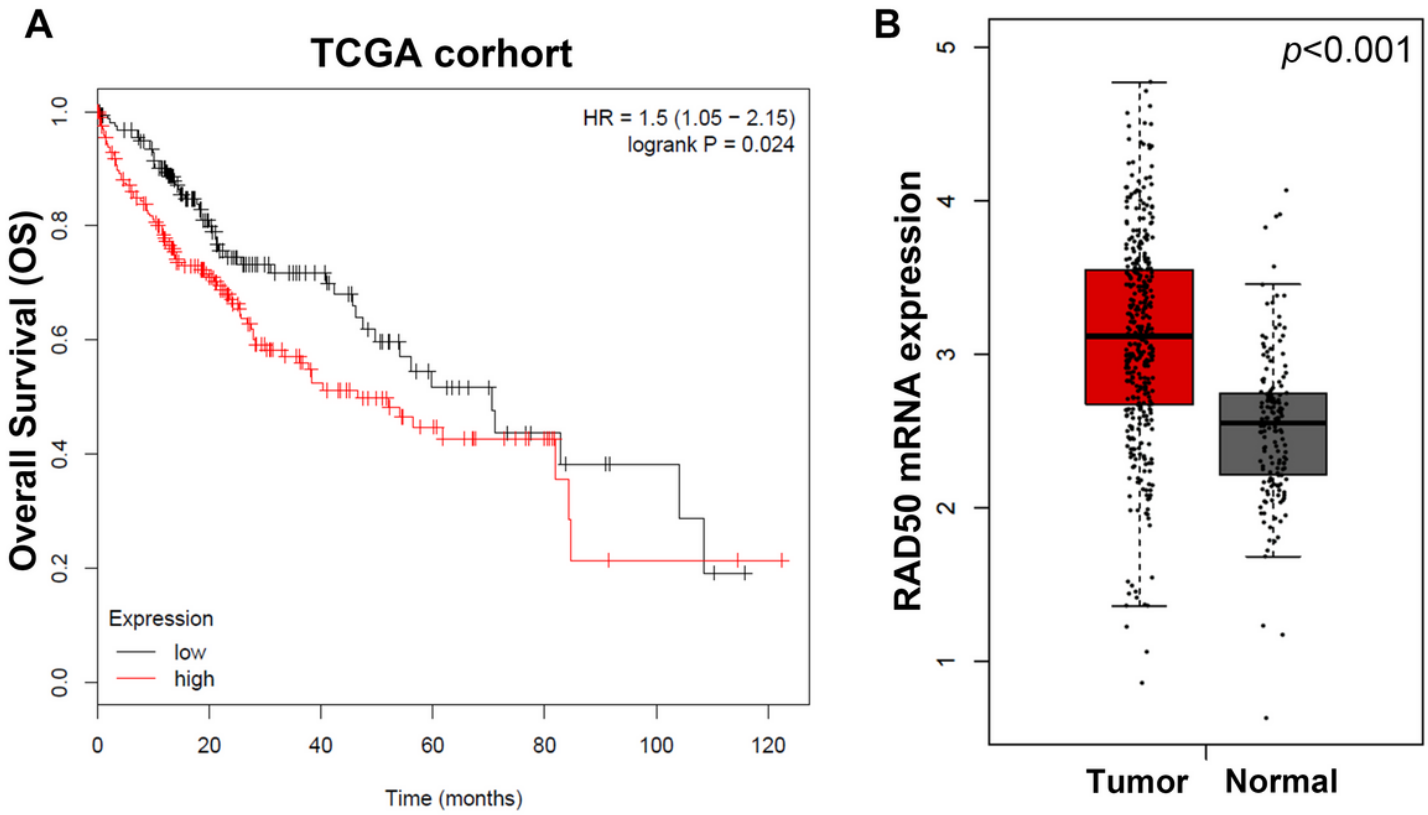

Figure 1

A: Kaplan-Meier survival analyses of different RAD50 expression groups based on OS in 423 patients with hepatocellular carcinoma from the TCGA database; B: Differential transcriptomic expression of RAD50 in tumour and normal tissues in the TCGA cohorts.

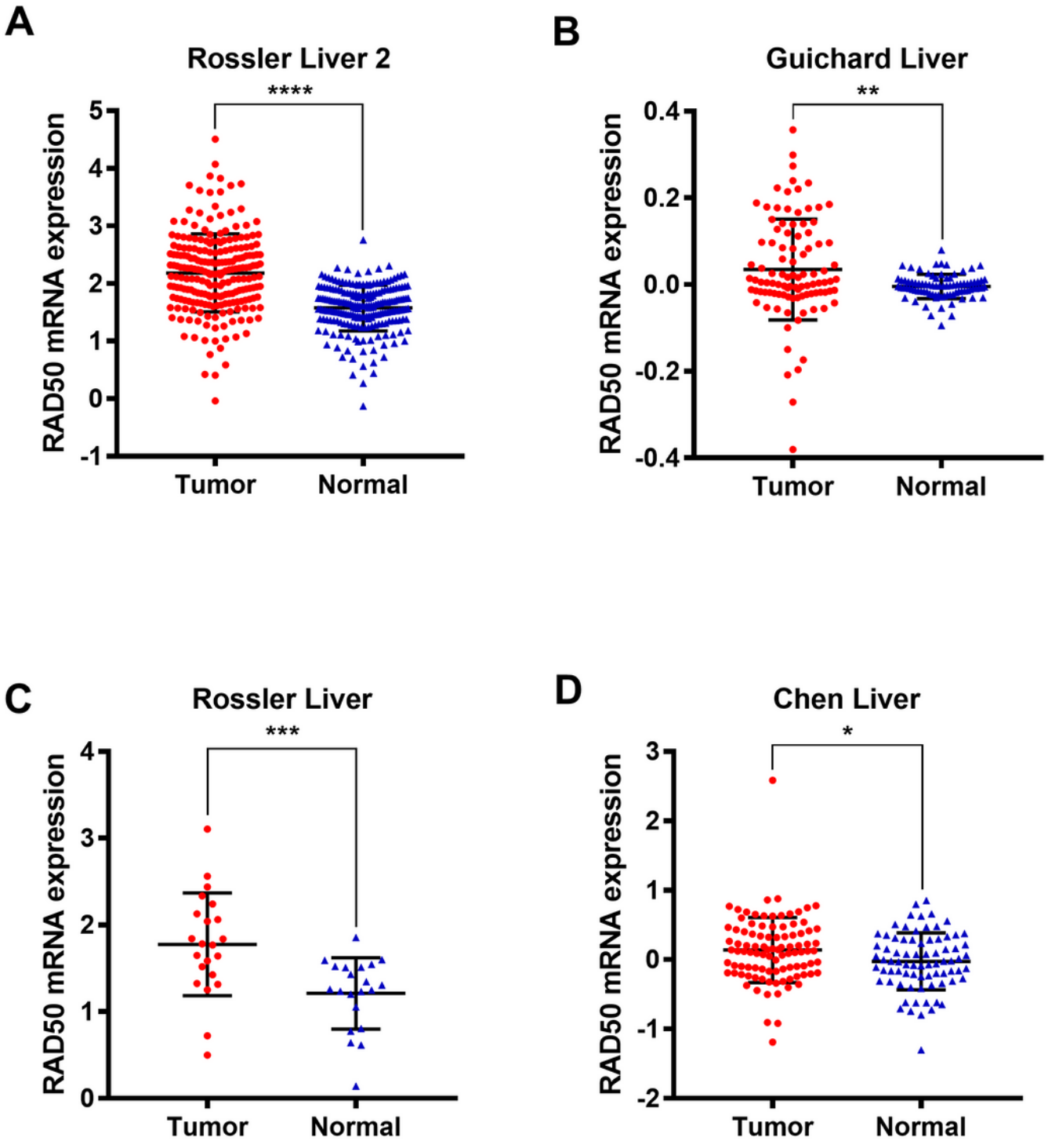

Figure 2

A: IHC staining of hepatocellular carcinoma and normal tissues from patients in the AHYMUN and AHNTU cohorts; B: Scatter plot showing the IHC scores derived from normal and tumour tissues ($p<0.001$) from different cohorts.

Figure 3

Forest plots were used to visualize the univariate Cox regression analysis of DFS and OS in the AHYMUM and AHNTU cohorts.

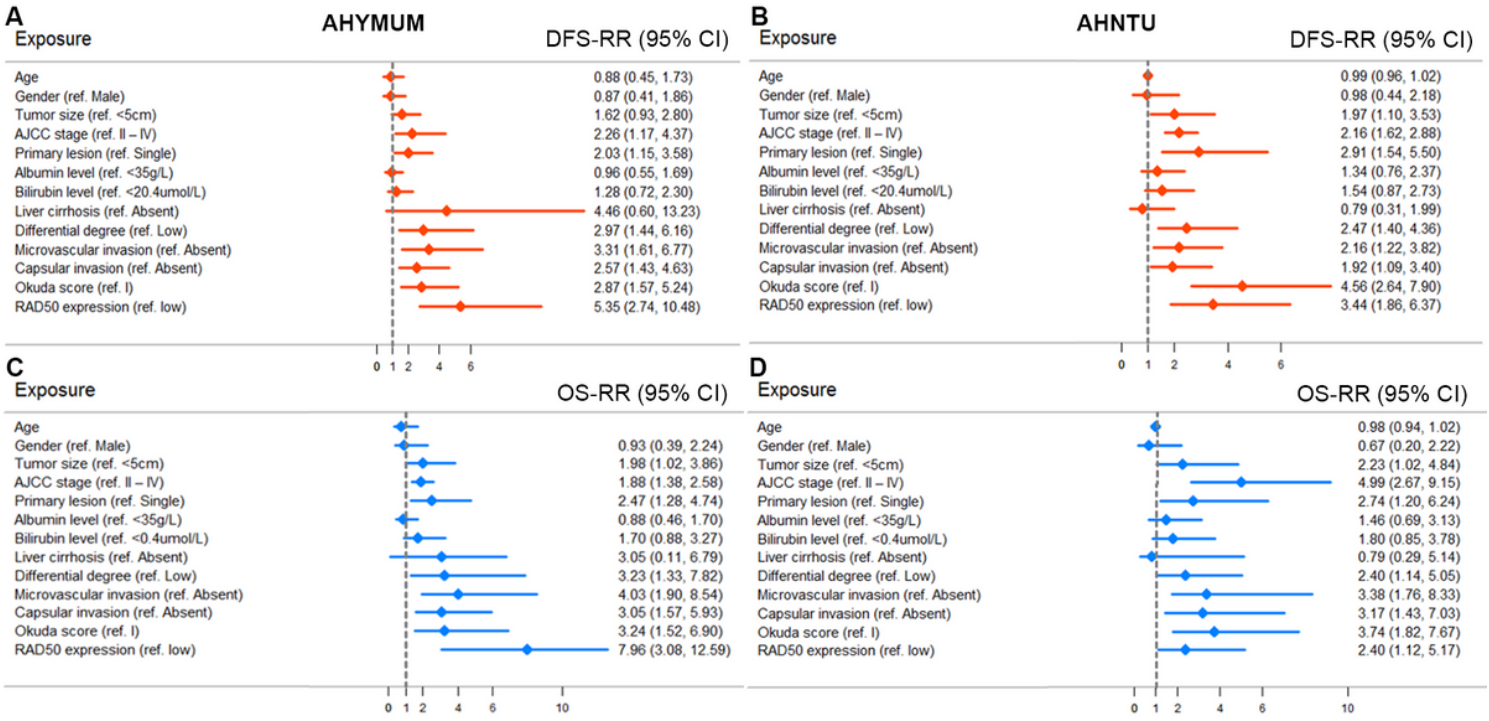

Figure 4

Kaplan-Meier survival analyses of different RAD50 expression groups based on OS and DFS in 107 patients with hepatocellular carcinoma from the AHYMUM cohort (A/B) and in 100 patients from the AHNTU cohort (C/D).

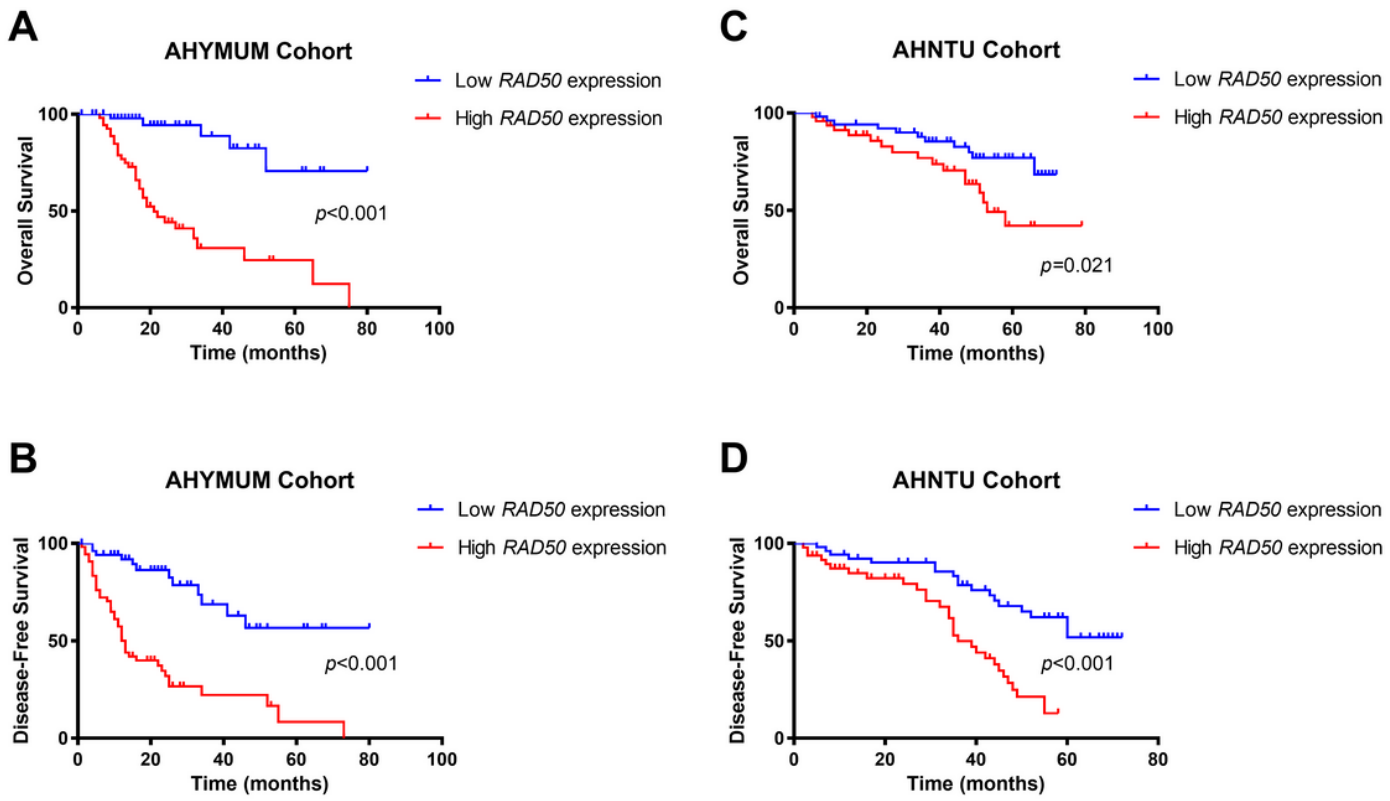

Figure 5

Analysis of expression in hepatocellular tumour vs. normal tissues based on data from the Oncomine database. (A) Roessler, et al., A unique metastasis gene signature enables prediction of tumor relapse in early-stage hepatocellular carcinoma patients, Cancer Res, 2010; (B) Guichard C, et al., Integrated analysis of somatic mutations and focal copy-number changes identifies key genes and pathways in hepatocellular carcinoma, Nature Genetics, 2012; (C) Roessler, et al., A unique metastasis gene signature enables prediction of tumor relapse in early-stage hepatocellular carcinoma patients, Cancer Res, 2010; (D) Chen X, et al., Gene expression patterns in human liver cancers, Mol Biol Cell, 2002.

Figure 6

Datasets from the TCGA database were analysed with the GSEA method. For each separate analysis, a Student's t-test was performed to obtained the statistical scores from the consistent pathways, and the means of the differential expression of genes were calculated. A permutation test was performed 1000 times to identify the significantly changed pathways. The adjusted P values (adj. P) were generated using the Benjamini and Hochberg (BH) false discovery rate (FDR) method by default and were used to correct for the occurrence of false positive results. Significantly related genes were defined by an adj. P less than 0.01 and an FDR less than 0.25. The most significant highly involved pathways included the nuclear body, ubiquitin ligase complex, G2M checkpoint and mitotic spindle pathways.

Supplementary Files

This is a list of supplementary files associated with this preprint. Click to download.

- supplement1.png
- supplement2.pdf